Acta Astronautica Vol. 12, No. 4, pp. 207–211, 1985
Printed in Great Britain.

0094–5765/85 $3.00 + .00

ORBITAL AND RELATIVE MOTION OF A TETHERED SATELLITE SYSTEM†

JOZEF C. VAN DER HA
European Space Operations Centre, Robert-Bosch-Str. 5, 6100 Darmstadt, F.R.G.

(*Received* 6 *January* 1984; *in revised form* 25 *May* 1984)

Abstract—A simplified model for the orbital and relative motion of a tethered satellite system is presented. The tether acts as a light elastic string with small structural damping but without bending stiffness. Its mass is taken into account in the calculation of the total kinetic and potential energies of the tethered system. This formulation allows the inclusion of the complete gravity gradient influence on the dynamics of the system. The resulting three-dimensional motion is separated in the centre of mass orbital motion on the one hand and the relative motion of the end-bodies on the other. No restrictions on length of the tether or on mass ratio of the end-masses are imposed. It is found that the frequencies and amplitudes of the longitudinal tether oscillations are realistic as long as the tether mass is less than that of the subsatellite.

1. INTRODUCTION

Tethered satellite systems are natural candidates for enhancing future Shuttle capabilities. They allow the deployment and retrieval of payloads down to orbits which cannot otherwise be considered due to high drag decay. Considerable potential is offered for deploying retrievable payloads with experiment facilities related to magnetospheric, atmospheric and microgravity sciences[1]. The dynamics of tethered satellite systems has received a great deal of interest over the last decade and at present fairly complete dynamical models are available.

In the ESA contract study conducted by Kohler *et al.*[2] the tether is considered as a thin continuum having bending as well as longitudinal stiffness (even torsional stiffness is analysed). The resulting equations of motion are in the form of partial differential equations with the motion of the end-masses as boundary conditions. Integration over time is performed after introducing a finite difference discretisation scheme along the tether. Another powerful model is presented by Misra and Modi[3] who also include the rotational motion of the end-bodies. The deployment and retrieval of the tether is far from straightforward (in particular the latter phase) and many sophisticated control procedures have been suggested, e.g. Kulla[4] and Spencer[5]. Many dynamical aspects of the tethered satellite systems, however, can be reproduced with sufficient accuracy by simplified tether models. This is illustrated by Kane and Levinson[6] who consider the relative motion as a succession of taut and slack phases where the transition through a taut phase is modelled as an instantaneous impact with an arbitrary coefficient of restitution reversing the direction of the relative velocity component along the tether. In the present paper another simplified model is presented in which the extended-tether phase is allowed to have a noninfinitesimal duration while the tether is modelled as a light elastic string with small structural damping. No restrictions on the length of the tether or on the ratio of the end-masses are imposed. The contribution of the tether mass to the system's kinetic and potential energies is taken into account in an approximate manner. The dynamics is separated in the orbital motion of the centre of mass and the relative motion of the end-masses relative to the local frame connected to the centre of mass. The coupling between relative and orbital motion is incorporated through a full expansion of the gravity-gradient effect. The only simplifying assumption consists of prescribing the centre of mass to be moving in an arbitrary orbit within a fixed plane. Perturbing effects such as air drag and Earth's oblateness may be taken into account in a similar manner as done in free-flying relative motion[7] in first approximation.

2. FUNDAMENTAL ASPECTS OF TETHERED SATELLITES MODEL

A three-dimensional tethered satellite configuration in orbit is considered. The end-masses are referred to as station and probe, i.e. idealised point-masses with positions $\underline{r}_s$ and $\underline{r}_p$ in the inertial X, Y, Z reference frame whose origin coincides with the centre of attraction. In our model it is assumed that the tether cross-section is sufficiently thin that bending and torsional stiffness can be neglected. Furthermore, inertial and perturbing forces acting along the tether are ignored. Under these assumptions the tether can be considered as a light elastic string capable of storing axial strain energy. For the purpose of evaluating the relative motion of the tethered probe with respect to the station the contributions of the tether mass to the system's potential and kinetic energies will be taken into account which results in a two-lumped-masses model for the tethered satellite dynamics. The model assumes that at all times the tether mass is distributed uniformly along the line connecting station and probe, i.e. along the vector $\underline{r} = \underline{r}_p - \underline{r}_s$ in Fig. 1. This

†Paper presented at the 34th Congress of the International Astronautical Federation, Budapest, Hungary, 9–15 October 1983.

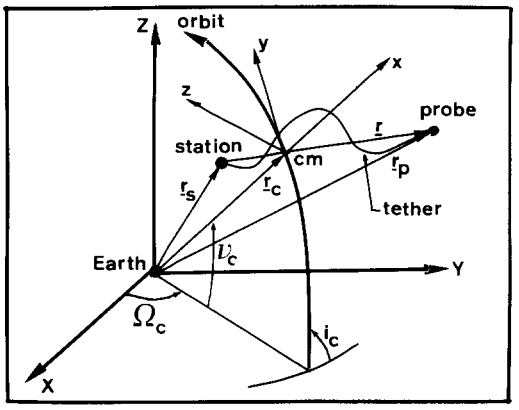

Fig. 1. Geometry of tethered satellite system.

simplification appears sufficiently realistic as long as the tether is stretched. In the case when the tether is slack there may at times be significant deviations between actual and assumed mass distributions. Nevertheless, the kinetic and potential energies calculated on this basis should be representative for the actual values in a mean sense. Furthermore, the assumed mass distribution is the only practical one apart from going into the detailed dynamics of the tether mass elements.

2.1 *Position of centre of mass*

Under the assumptions stated above the centre of mass position $\underline{\mathbf{r}}_c$ within the inertial frame is obtained by integrating the contributions of the tether mass elements along the vector $\underline{\mathbf{r}}$ as follows:

$$\underline{\mathbf{r}}_c = \{m_s\underline{\mathbf{r}}_s + m_p\underline{\mathbf{r}}_p + m_t\int_0^1 (\underline{\mathbf{r}}_s + s\underline{\mathbf{r}})\, ds\}/m$$
$$= \{\underline{\mathbf{r}}_s + \kappa\underline{\mathbf{r}}_p\}/(1 + \kappa),$$

with

$$\kappa = (m_p + m_t/2)/(m_s + m_t/2). \tag{1}$$

Here, m_s, m_p, m_t represent the masses of station, probe and tether, respectively, whereas m stands for the sum of these masses. The parameter κ denotes the mass-ratio of the two lumped masses. For a typical tether the mass density is of the order of 1 kg/km so that the tether mass would usually be less than any of the end-masses.

2.2 *Total kinetic energy*

In order that the assumed system configuration is conserved as time progresses, it is obvious that the velocity of the modelled tether mass elements must vary linearly in the range from $\underline{\mathbf{v}}_s$ to $\underline{\mathbf{v}}_p$ along the line connecting the station and probe: $\underline{\mathbf{v}}(s) = (1 - s)\underline{\mathbf{v}}_s + s\underline{\mathbf{v}}_p$ for $0 < s < 1$. The total kinetic energy is obtained by integrating the contributions of the tether elements along the vector $\underline{\mathbf{r}}$:

$$T = \frac{1}{2}(m_s + m_t/3)\, v_s^2 + \frac{1}{2}(m_p + m_t/3)\, v_p^2 + \frac{1}{6} m_t\, (\underline{\mathbf{v}}_p, \underline{\mathbf{v}}_s). \tag{2}$$

This result can be simplified by expressing the velocities $\underline{\mathbf{v}}_s$ and $\underline{\mathbf{v}}_p$ in terms of the velocity of the centre of mass, i.e. $\underline{\mathbf{v}}_c = (\underline{\mathbf{v}}_s + \kappa\underline{\mathbf{v}}_p)/(1 + \kappa)$, and the relative velocity vector $\underline{\mathbf{v}} = \underline{\mathbf{v}}_p - \underline{\mathbf{v}}_s$:

$$\underline{\mathbf{v}}_s = \underline{\mathbf{v}}_c - \kappa\underline{\mathbf{v}}/(1 + \kappa),$$
$$\underline{\mathbf{v}}_p = \underline{\mathbf{v}}_c + \underline{\mathbf{v}}/(1 + \kappa). \tag{3}$$

The total kinetic energy expression in eqn (2) takes now the very compact form:

$$T = \frac{1}{2} m v_c^2 + \frac{1}{2}(\bar{m} - m_t/6)v^2, \tag{4}$$

where m is the total mass and $\bar{m}$ is the so-called "reduced mass" of the tether system:

$$\bar{m} = (m_p + m_t/2)(m_s + m_t/2)/m$$
$$= \kappa m/(1 + \kappa)^2. \tag{5}$$

The former term in eqn (4) represents the kinetic energy of the motion of the centre of mass whereas the latter term describes the motion of the system around the centre of mass. The result of eqn (4) contains a number of interesting special cases (e.g., a rotating thin rod in orbit) which allow us to confirm its validity.

2.3 *Total gravitational potential energy*

The total gravitational potential energy consists of the contributions of station, probe and tether. The latter is obtained by integration over the line connecting the probe and station. The position vectors of station and probe expressed in terms of the position vector of the centre of mass of eqn (1) and the relative position vector $\underline{\mathbf{r}} = \underline{\mathbf{r}}_p - \underline{\mathbf{r}}_s$ are given as follows:

$$\underline{\mathbf{r}}_s = \underline{\mathbf{r}}_c - \kappa\underline{\mathbf{r}}/(1 + \kappa),$$
$$\underline{\mathbf{r}}_p = \underline{\mathbf{r}}_c + \underline{\mathbf{r}}/(1 + \kappa). \tag{6}$$

Under the assumption of uniform mass distribution on the line connecting probe and station the position vector of a tether mass element can be written as:

$$\underline{\mathbf{r}}\,(s) = \underline{\mathbf{r}}_c + s\underline{\mathbf{r}},$$
$$-\kappa/(1 + \kappa) < s < 1/(1 + \kappa). \tag{7}$$

The total gravitational potential energy of the tethered satellite system is given by the expression

$$V_g = -\mu\{m_s/r_s + m_p/r_p + m_t\int ds/|\underline{\mathbf{r}}_c + s\underline{\mathbf{r}}|\}, \tag{8}$$

where μ is the central body's gravitational parameter and the integration interval of s is given in eqn (7). In order to obtain an explicit expression, one makes use of the expansion in terms of Legendre polynomials P_j:

$$|\underline{\mathbf{r}}_c + s\underline{\mathbf{r}}|^{-1} = r_c^{-1}\,[1 + \sum_{j=1}^{\infty} (-sr/r_c)^j\, P_j(\xi)],$$
$$\xi = (\underline{\mathbf{r}}_c, \underline{\mathbf{r}})/(r_c r). \tag{9}$$

Similar expansions can naturally be used for $1/r_s$ and $1/r_p$. After integration over s and rearrangement of terms using the definition of κ in eqn (1) the resulting potential energy can be expressed in the form:

$$V_g = -(\mu/r_c)[1 + \sum_{j=1}^{\infty} M_j(r/r_c)^j P_j(\xi)],$$

with

$$M_j = \frac{1}{2}\{(2m - m_t)[\kappa^j + \kappa(-1)^j] - m_t(j-1) \times [\kappa^{j+1} + (-1)^j]/(j+1)\}/(1+\kappa)^{j+1}. \quad (10)$$

It is seen that the coefficient M_1 vanishes which is due to the definition of the centre of mass as given in eqn (1). The first few nonvanishing terms can be simplified considerably when expressed in terms of the reduced mass $\bar{m} = \kappa m/(1+\kappa)^2$ and m_t:

$$M_2 = \bar{m} - m_t/6; \quad M_3 = (\kappa - 1)(\bar{m} - m_t/4)/(1+\kappa). \quad (11)$$

It is of interest to note that M_2 coincides with the mass-coefficient multiplying the relative velocity component of the kinetic energy expression in eqn (4). In the case when $\kappa = 1$, i.e. $m_p = m_s$, all odd coefficients M_j in eqn (10) will vanish.

2.4 *Strain energy of tether*

Because of the underlying assumptions of the present analysis the only structural potential energy to be taken into account is the strain energy related to the axial extension of the tether. In the case that the tether can be assumed to be uniformly deformed (i.e. the displacement of any reference point on the undeformed tether is proportional to its distance from the attachment point) the strain energy of the tether takes the same mathematical form as the potential energy of a massless spring:

$$V_s = \frac{1}{2} k (r - l)^2; \quad k = AE/l. \quad (12)$$

Here, A and l are the cross-sectional area and length of the undeformed tether whereas E stands for the tensional elasticity modulus of the tether material. During the intervals when the tether is slack the strain energy should be taken zero, i.e. $V_s = 0$ for $r < l$. The frequency of the axial oscillations of the corresponding free mass-spring system would be given by:

$$\omega = [k/(\bar{m} - m_t/6)]^{1/2}, \quad r > l; \quad \omega = 0, \quad r < l, \quad (13)$$

where the effective reduced mass appearing here also takes account of the effect of tether mass on the axial frequency.

For typical tether materials (e.g., Aramid) with a longitudinal stiffness AE in the neighbourhood of 10^4N and a typical tether configuration with l in the range of 10–100 km and $\bar{m}$ from 100–1000 kg the tether's axial frequency ranges from about 10–100 times the orbital frequency. As can be seen from eqns (12) and (13) the frequency increases with decreasing tether length and decreasing reduced mass.

2.5 *Structural damping of tether*

Due to the internal structural friction of the tether material, strain energy is dissipated and successive amplitudes of the longitudinal extensions will decay slowly. This effect is known as hysteresis damping and may be described in a quantitative mathematical form by introducing an "equivalent" viscous damping phenomenon. The equivalence is based on the fact that the viscous damping coefficient is taken such that the corresponding amplitude decrements are identical. In the present application the structural damping of the tether can therefore be described by means of Rayleigh's dissipation function for viscous damping:

$$F = \frac{1}{2} d\dot{r}^2 = (\bar{m} - m_t/6)\xi\omega\dot{r}^2, \quad (14)$$

where ξ is the damping factor (relative to critical damping) and ω is the free axial frequency of eqn (13). In the case that $r < l$ the damping vanishes together with ω. The damping factor is not more than a few percent for tether materials under consideration.

3. EQUATIONS OF MOTION OF TETHERED SYSTEM

The equations of motion of the tethered satellite system are to be derived from the fundamental energy expressions derived above. It is important to recognise that the complete motion of the tethered system considered here is described by the vectors $\underline{\mathbf{r}}_c$, $\underline{\mathbf{v}}_c$ and $\underline{\mathbf{r}}$, $\underline{\mathbf{v}}$ since the position and velocity vectors of both station and probe can be expressed in these quantities as shown in eqns (3) and (6).

3.1 *Motion of the centre of mass*

The actual motion of the centre of mass is extremely complicated if all perturbations acting on the tether system are to be considered. The assumption on the position and velocity vectors of the centre of mass mentioned above implies that its acceleration is given by

$$\ddot{\underline{\mathbf{r}}}_c = (\ddot{\underline{\mathbf{r}}}_s + \kappa\ddot{\underline{\mathbf{r}}}_p)/(1+\kappa) = -\mu\underline{\mathbf{r}}_c/r_c^3[1 + O(r^2/r_c^2)] + (\underline{\mathbf{F}}_s + \underline{\mathbf{F}}_p)/m. \quad (15)$$

Here, $\underline{\mathbf{F}}_s$ and $\underline{\mathbf{F}}_p$ represent the perturbing forces acting on the station and probe taken as lumped masses $m_s + m_t/2$ and $m_p + m_t/2$. The form of eqn (15) suggests that the centre of mass can be considered to be moving in a perturbed orbit with instantaneous orbital plane defined by the osculating $\underline{\mathbf{r}}_c$ and $\dot{\underline{\mathbf{r}}}_c$ vectors. The essential advantage in considering the centre of mass (rather than say the station) as reference for the relative motion is based on the fact that the resulting restoring and damping forces acting along the tether axis have no effect on the acceleration of the centre of mass as can be seen from eqn (15). Of particular interest is the evolution of the

local x, y, z reference frame with x, y axes along the local vertical and horizontal of the centre of mass and the z-axis normal to its orbital plane. (Fig. 1). The motion of this frame with respect to inertial space is described by the rotation vector $\underline{\dot{v}}_c$ which has a small component along the instantaneous x axis due to the out-of-plane "perturbing" force component of eqn (15). The axial tether forces do not contribute to this effect and the gravity gradient influence in this regard is negligibly small when $r << r_c$ so that mainly external perturbations (e.g. oblateness) can be responsible for orbital plane changes. In the present analysis the orbital plane of the centre of mass is considered fixed in inertial space so that the rotation vector $\underline{\dot{v}}_c$ is pointing along the local z axis. This means that the motion of the centre of mass can be described by only two generalised coordinates, i.e. the polar coordinates r_c and v_c.

3.2 *Equations of motion*

The relative motion with respect to the local frame connected with the centre of mass is described most conveniently by the generalised coordinates r, ϕ and ψ. The range r is the relative distance between station and probe whereas ϕ and ψ are the in-plane and out-of-plane Euler angles describing the orientation of the vector $\underline{\mathbf{r}}$ in the local frame (Fig. 2). After expressing the relative velocity $\underline{\mathbf{v}}$ in terms of the chosen coordinates the kinetic energy expression of eqn (4) becomes:

$$T = \frac{1}{2} m (\dot{r}_c^2 + r_c^2 \dot{v}_c^2) + \frac{1}{2} (\bar{m} - m_t/6) \times [\dot{r}^2 + r^2\dot{\psi}^2 + r^2(\dot{v}_c + \dot{\phi})^2 \cos^2\psi]. \quad (16)$$

The total gravitational potential energy given in eqn (10) is already expressed in the right form except for ξ which equals $\cos\psi \cos\phi$. The five equations of motion follow now from the Lagrange formalism taking account of the dissipation function of eqn (14) and the generalised perturbing forces Q_j:

$$\ddot{r}_c - r_c\dot{v}_c^2 + (\mu/r_c^2)\,[1 + \sum_{j=2}^{\infty} (j+1)\,(M_j/m) \times (r/r_c)^j P_j(\xi)] = Q_c/m,$$

$$\frac{d}{dt}\,[m r_c^2 \dot{v}_c + (\bar{m} - m_t/6) r^2 (\dot{v}_c + \dot{\phi}) \cos^2\psi] = Q_v,$$

$$\ddot{r} - r[\dot{\psi}^2 + (\dot{\phi} + \dot{v}_c)^2 \cos^2\psi] + 2\zeta\omega\dot{r} + \omega^2 (r - l) = Q_r/M_2 + (\mu/r_c^2) \sum_{j=2}^{\infty} j\,(M_j/M_2)(r/r_c)^{j-1} P_j(\xi),$$

$$\ddot{\phi} + \ddot{v}_c + 2(\dot{\phi} + \dot{v}_c)(\dot{r}/r - \psi\tan\psi) = Q_\phi/M_2 - (\mu/r_c^3)(\sin\phi/\cos\phi) \sum_{j=2}^{\infty} (M_j/M_2)(r/r_c)^{j-2} P_j'(\xi),$$

$$\ddot{\psi} + 2\dot{r}\dot{\psi}/r + (\dot{\phi} + \dot{v}_c)^2 \sin\psi \cos\psi = Q_\psi/M_2 - (\mu/r_c^3) \sin\psi \cos\phi \sum_{j=2}^{\infty} (M_j/M_2)(r/r_c)^{j-2} P_j'(\xi). \quad (17)$$

These equations contain the complete expansion of the gravity-gradient perturbing effects on all coordinates. The second equation expresses the conservation of angular momentum in the absence of external torques. It is seen that orbital momentum and "relative" momentum can be exchanged. In the case $\psi = \pm\pi/2$ a singularity in the equation for ϕ appears as it becomes undefined and a different form of the equations should be used. As this case corresponds to a hypothetical situation no difficulties are expected in most applications. In the planar case, ψ and $\dot{\psi}$ vanish and the equations of motion become much simpler. Another important special case occurs when the tether length is much smaller than the orbital distance so that terms of order $(r/r_c)^2$ can be ignored. In that case, the centre of mass radial motion can be considered uncoupled from the tether's gravity-gradient influence and the tether's angular momentum can be considered negligible with respect to the orbital momentum. The tether dynamics for small r/r_c and in-plane motion is described by:

$$\ddot{r} - r(\dot{\phi} + \dot{v}_c)^2 + 2\zeta\omega\dot{r} + \omega^2(r - l) = Q_r/M_2 + \mu r(3\cos^2\phi - 1)/r_c^3,$$

$$\ddot{\phi} + 2(\dot{\phi} + \dot{v}_c)\dot{r}/r + \ddot{v}_c = Q_\phi/M_2 - 3\mu \sin\phi\cos\phi/r_c^3. \quad (18)$$

These simplified equations illustrate that for small variations in the range r the in-plane oscillations due to gravity-gradient effects are essentially governed by the familiar nonlinear pendulum equation. Also it is seen that deployment (i.e. $\dot{r} > 0$) leads to damping of the in-plane oscillations whereas retraction (i.e. $\dot{r} < 0$) results in negative damping which may cause instabilities. Furthermore, it is found that for small in-plane angle and rate the frequency of the axial motion under tension is approximately $(\omega^2 - 3\dot{v}_s^2)^{1/2}$ where a near-circular orbit is assumed. This means that the orbital motion tends to reduce the axial tether frequency in this case. In order that the tether's stiffness is able to withstand the gravity-gradient pull ω must be larger than $\sqrt{3}$ times the orbital frequency. After transition from taut to slack phase, a fully different dynamic behaviour of the system appears as it is essentially moving under the free gravitational influence which tends to drive the masses apart in most cases.

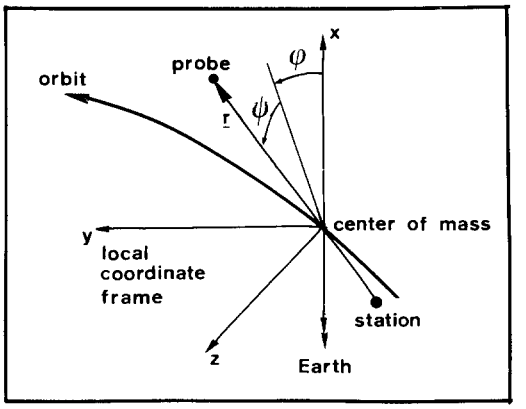

Fig. 2. Visualisation of Euler angles ϕ, ψ.

4. DISCUSSION OF RESULTS

The validity of the approximate tether model has been evaluated by comparison with the continuum model of

Kohler *et al.*[2]. In their first example (Chap. 6) a Shuttle orbit with perigee and apogee distances of 200 and 1000 km is considered. The mass of Shuttle and probe is taken as 10^5 and 200 kg. The tether has an undeformed length of 100 km and mass density of 1 kg/km. Its longitudinal stiffness is taken as $AE = 1500$ N. Initially the Shuttle is at perigee and the tether is stretched downwards along the local vertical with a strain of 7%. The resulting relative motion consists of a low frequency (once per orbit) oscillation due to gravity-gradient variations induced by the Shuttle's orbital eccentricity. Superimposed on this motion is a higher frequency (about 8 times per orbit) component due to the axial oscillations of the tether. The amplitudes of the oscillations are of the order of 2.5 and 0.4 km, respectively, so that the tether remains under tension. The frequencies of the relative motion oscillations are predicted correctly by the present model.

The large amplitude variations are identical to within a few percent but the small amplitude of the high-frequency motion is consistently too low. This is caused by the fact that the tension acting on the probe is slightly oversized in the near-equilibrium situation of axial restoring and gravity gradient forces of the present example. Nevertheless, the trends in the ratios of the successive maximum and minimum deflections are completely preserved. The extrema of the tether tension over the first orbit are predicted as 111 and 63 N which may be compared with the extrema of the averaged tension along the tether of reference [2] of 113 and 56 N. Naturally the reliability of the high-frequency amplitude prediction should be expected to deteriorate further when the tether mass increases with respect to that of the probe.

Finally, an illustration of a successful passive deployment of a tethered satellite is given in Fig. 3. In this case, oblateness and air drag perturbations acting on both end-masses are taken into account. Because of the relative dominance of the tether forces the effects of these perturbations (even for high exospheric temperature and large difference in ballistic parameters of probe and station) on the evolution of the range are not very pronounced and could hardly be observed on the scale used in Fig. 3.

In the results shown, the probe is released with a relative velocity of 2.8 m/sec in a direction opposite to the Shuttle's velocity vector. The initial impulse has been chosen on the basis of the Clohessy–Wiltshire free relative motion relations such that the 10 km long tether becomes taut for the first time a little before it would start reversing its motion. A damping of 3% is taken which leads to full deployment after about 2.5 orbits. The subsatellite oscillates downwards from the Shuttle within an angle of about 30° from the local vertical. These oscillations are hard to damp passively. The maximum tension occurs during the first stretching and amounts to about 105 N. Because of its heavy mass the Shuttle's orbital motion is hardly affected by the tether forces: its radial distance changes by just a few tens of meters under this effect. Of similar magnitude is the amplitude of the out-of-plane oscillations induced by the differential oblateness perturbations on the two end-masses.

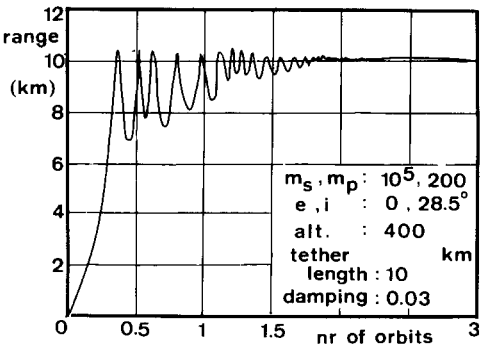

Fig. 3. Evolution of range under passive deployment to local vertical.

5. CONCLUSIONS

The simplified model presented here should be useful in the prediction of tethered satellites relative motion as well as in the assessment of the dynamical interaction with the orbital motion. In particular, the feasibility of passive deployment schemes and the maximum loads acting on the tether material can be predicted with sufficient accuracy in many applications. Since a full gravity-gradient expansion is included in the model full accuracy is retained also for long tethers. In cases where the tether mass is substantial relative to the end-masses degradation of the accuracy of the high-frequency amplitude prediction in a near-equilibrium situation should be expected.

REFERENCES

1. I. Bekey, Tethers open new space options. *Astronaut. Aeronaut.* **21**, 32–40 (1983).
2. P. Kohler, W. Maag and R. Wehrli, Dynamics of a system of two satellites connected by a deployable and extensible tether of finite mass. *ESA-CR(P)*-1205 (1978).
3. A. K. Misra and V. J. Modi, A general model for the Space Shuttle-based tethered subsatellite system. *Advances Astronaut. Sci.* **40**, 537–557 (1979).
4. P. Kulla, Dynamics of tethered satellites. ESA Symp. Dynam. Contr. Non-Rigid Spacecraft, *ESA-SP*-117, 349–354 (1976).
5. T. M. Spencer, Atmospheric perturbations and control of a Shuttle-tethered satellite. *Automatica* **16**, 629–636 (1980).
6. T. R. Kane and D. A. Levinson, Deployment of a cable-supported payload from an orbiting spacecraft. *J. Spacecraft Rockets* **14**, 409–413 (1977).
7. J. C. Van der Ha, Three-dimensional subsatellite motion. *Celest. Mech.* **26**, 285–309 (1982).